



Lung cancers associated with cystic airspaces: CT features and pathologic correlation

Yingran Shen^{a,1}, Xinnan Xu^{a,1}, Yunfei Zhang^{a,2}, Weitong Li^{c,2}, Jie Dai^{a,3}, Siming Jiang^{a,3}, Tong Wu^b, Haomin Cai^a, Alan Sihoe^a, Jingyun Shi^{b,*,*}, Gening Jiang^{a,*}

^a Department of Thoracic Surgery, Shanghai Pulmonary Hospital, Tongji University, Shanghai, 200433, China

^b Department of Medical Imaging, Shanghai Pulmonary Hospital, Tongji University, Shanghai, 200433, China

^c Department of Medical Imaging, Shishi Hospital, Fujian, 362700, China

ARTICLE INFO

Keywords:

Lung adenocarcinoma
Computed tomography
Histological types of neoplasms

ABSTRACT

Objective: Lung cancer associated with cystic airspaces (LCCA) is a rare entity. The diagnosis and treatment is often delayed due to lack of comprehension of this disease. We aimed to elucidate LCCA's clinicopathological characteristics and investigate imaging features correlated with pathological invasiveness.

Method: The preoperative computed tomographic (CT) scans of 10,835 patients diagnosed with NSCLC between January 2015 and December 2016 were reviewed by two thoracic radiologists for association with a cystic airspace. A clinicopathological and radiological feature analysis was done.

Result: A total number of 123 LCCA patients were identified and four morphologic patterns were recognized: I, thin-walled type (n = 23, 18.7%); II, thick-walled type (n = 34, 27.6%); III, a cystic airspace with a mural nodule (CWN) type (n = 43, 35.0%); and IV, mixed type (n = 23, 18.7%). A solid component in the cyst wall predicted histological invasiveness in all four types of LCCA. The proportion of moderately/poorly (M/P)-differentiated subtype in type III (85.0%) was higher than in other three patterns (which were 50.0%, 50.0%, and 69.6%, respectively). Multivariate analysis revealed that type III pattern (odds ratio [OR], 6.5; 95% confidence interval [CI], 1.1–36.4; P = 0.035), part-solid/solid component in wall (part-solid: OR, 27.2; 95% CI, 5.6–3131.6; P < 0.001; solid: OR 614.6; 95% CI, 36.4–10,368.6; P < 0.001), and irregular inner surface of cyst (OR 7.0; 95% CI 1.9–26.2; P = 0.004) were independent risk factors for the M/P-differentiated subtype. EGFR mutations were the predominant genetic alterations in each type of LCCAs, but no significant difference was found among them.

Conclusions: In LCCA, morphological patterns and wall components were two important predictors for determining pathological invasiveness.

1. Introduction

The definition of cystic airspace was first standardized by the

Fleischner Society in 1996 [1] and was described as an enlarged unit of peripheral air-containing lung that was surrounded by a wall of variable thickness. This definition was updated in 2009 [2]. Cystic airspace-

Abbreviations: LCCA, lung cancer associated with cystic airspaces; CWN, a cystic airspace with a mural nodule; M/P, moderately/poorly; OR, odds ratio; CI, confidence interval; AIS, adenocarcinoma *in situ*; MIA, minimally invasive adenocarcinoma; SD, standard deviation; IQR, interquartile range; SCC, squamous cell carcinoma; HU, hounsfield units

* The abstract of this manuscript was selected by the Programme Committee for presentation at the 32nd EACTS Annual Meeting, 18–20 October 2018, in Milan, Italy.

* Corresponding author at: Department of Thoracic Surgery, Tongji University Affiliated Shanghai Pulmonary Hospital, No. 507 Zhengmin Road, Shanghai, 200433, China.

** Corresponding author at: Department of Medical Imaging, Tongji University Affiliated Shanghai Pulmonary Hospital, No. 507 Zhengmin Road, Shanghai, 200433, China.

E-mail addresses: shijingyun89179@126.com (J. Shi), jgnwp@aliyun.com (G. Jiang).

¹ Yingran Shen and Xinnan Xu contributed equally to the paper.

² Yunfei Zhang and Weitong Li contributed equally to the paper.

³ Jie Dai and Siming Jiang contributed equally to the paper.

<https://doi.org/10.1016/j.lungcan.2019.05.012>

Received 2 February 2019; Received in revised form 23 April 2019; Accepted 6 May 2019

0169-5002/ © 2019 Published by Elsevier B.V.

related abnormalities differ among cases and include emphysematous bullae, congenital or fibrotic cysts, subpleural blebs, bronchiectatic airways, and distended distal airspaces [3], most of which are indicative of benign lesions. Lung cancers associated with cystic airspaces (LCCAs) have been described as uncommon [1]. The relative infrequency of these cancers explains why there is no specific algorithm for a workup of these lesions in standardized management protocols. However, this appearance has been increasingly identified in lung cancer screening programs. Data from the International Early Lung Cancer Action Program (IELCAP) showed that 3.7% (26/706) of lung cancers presented this specific computed tomographic (CT)-based morphology [4]. In the Netherlands-Leuven Longkanker Screenings Onderzoek (NELSON) lung cancer screening trial, lung LCCAs accounted for 22.7% of missed or delayed cancer diagnoses [5].

A definitive tissue-based LCCA diagnosis can be difficult in cases in which the lesions are small. Surrounding cystic areas render patients at high risk for biopsy-related complications, such as pneumothorax, and also pose diagnostic challenges for lung cancer [3]. In this case, morphological assessment via thin-section CT has taken on greater importance.

In this article, we reviewed clinicopathological characteristics in LCCA patients and evaluated their CT morphological features. In addition, the correlation between imaging features and pathological invasiveness was investigated.

2. Materials and methods

2.1. Patient selection

Two experienced chest radiologists (Weitong Li, chief radiologist, 20 y of experience; Tong Wu, attending radiologist, 7 y of experience) retrospectively and independently reviewed all consecutive patients who had undergone curative-intent surgery and were diagnosed with NSCLC between January 2015 and December 2016 in our institution with the aim of identifying LCCAs. Any discrepancies in their evaluations were reviewed by another senior reader (Jingyun Shi, chief radiologist, 27 y of experience) and resolved through consensus.

Surgery was performed only when complete resection could be achieved. For patients preoperatively diagnosed as multiple level node (N)2, induction treatment was applied, and surgery was considered only if mediastinal downstaging was achieved. Mediastinal lymph node dissection consisted of complete resection of all nodes at stations 2, 4, and 7–10R for right-sided tumors and nodes at stations 4–10L for left-sided tumors.

A cystic airspace was defined as a round parenchymal lucency consisting of a well-defined interface with the normal lung [2]. The following exclusion criteria applied: (a) airspace in the center of a previously solid lesion suggesting cavitation and (b) the airspace cannot be differentiated from surrounding emphysema, bronchiectasis, or cystic interstitial lung disease [6]. As a result, 123 LCCA patients were identified from 10,835 surgical lung cancer cases.

Complete resection was achieved in all of these patients, and excised lymph nodes were collected and recorded according to Naruke's system [7]. Systematic nodal dissection was performed in a routine manner.

The clinicopathological features, including age at surgery, gender, pathological tumor–node–metastasis (TNM) stage (8th edition of the lung cancer staging system), histological subtype (World Health Organization Classification 2015), surgical procedure, and gene mutation status were obtained from the medical records. Mutation of epidermal growth factor receptor (EGFR), anaplastic lymphoma kinase (ALK) and kirsten rat sarcoma viral oncogene homolog (KRAS) were detected by the amplification-refractory mutation system (ARMS) real-time polymerase chain reaction (qPCR) kit (Beijing ACCB Biotech Ltd, TB002). For the detection of EGFR and KRAS mutation, genomic DNA was used. For the detection of ALK fusion, mRNA was first reverse-transcribed to cDNA. All detections were carried out following the

manufacturer's protocol.

2.2. Image analysis

All CT examinations were performed using two CT scanners (Brilliance, Philips Medical Systems Inc, Cleveland, the US and SOMATOM Definition AS, Siemens Aktiengesellschaft, Munich, Germany) and were evaluated on the IntelliSpace Portal workstation with a fixed window setting (width, 1400; level, –500). CT parameters of Brilliance were as follows: (a) tube voltage, 120 kV; (b) tube current, 180 mA; (c) acquisition, 64×1 mm; (d) rotation time, 0.75 s; (e) Pitch: 0.906; (f) FOV: 350 mm; (g) reconstruction thickness, 2 mm and (h) reconstruction interval, 1 mm. CT parameters of SOMATOM Definition AS were as follows: (a) tube voltage, 120 kV; (b) tube current, 180 mA; (c) acquisition, 128×0.6 mm; (d) rotation time, 0.5 s; (e) Pitch: 1.2; (f) FOV: 300 mm; (g) reconstruction thickness, 2 mm and (h) reconstruction interval, 1 mm.

Qualitative data included bronchial margins, presence of air bronchogram or pleural tag, component of cyst wall, inner surface of cyst, locule within cyst and location of nodule. Margins were classified as predominantly smooth, spiculated and/or lobulated. The air bronchogram was defined as a pattern of air-filled (low-attenuation) bronchi on a background of an opaque (high-attenuation) airless lung [2]. The pleural tag represented visceral pleura pulling toward the pulmonary nodule [8]. The wall component was categorized as pure ground glass, part-solid, and solid. The inner surface of the cyst was classified as smooth or irregular. The locules within the cyst were categorized as unilocular or multilocular based on the number of locules. We defined the peripheral lung area as the outer third of the lung and the central lung area as the inner two thirds of the lung.

Quantitative measurements included cyst size, wall thickness, CT value of wall/whole lesion/nodule, the largest diameter of the whole lesion/nodule, and volume of the whole lesion/nodule. Cyst size was represented by the cross section measurement across the widest part of the cyst (a product of the longest diameter of the cystic airspace and the axis perpendicular to it). The largest nodule diameter and volume could be directly obtained from the workstation. Four segments evenly distributed on the wall of the largest section were taken for measuring and calculating the cyst's average thickness and CT-measured wall density.

2.3. Classification of lung cancers based on CT morphology

LCCAs were classified by morphology based on preoperative CTs using a modified classification system based on previous studies by Mascaldi [9] and Fintelman [6] (Fig. 1). Type I (thin-walled type) indicated a cystic airspace with an average wall thickness < 2 mm, while type II (thick walled type) referred to those circumferential thickening cystic airspaces with mean wall thickness ≥ 2 mm. Type III (CWN type) denoted a cystic airspace with a mural nodule (either endophytic or exophytic). Type IV (mixed type) corresponded to solid or nonsolid tissue intermixed within clusters of multiple cystic airspaces.

2.4. Grouping of pathological subtypes

In the correlation analysis between imaging characteristics and pathological subtypes and after considering the number of patients and prognosis in each subtype, we excluded squamous cell carcinoma, and used two categories for adenocarcinoma classification in this study. We classified adenocarcinoma *in situ* (AIS), minimally invasive adenocarcinoma (MIA), and lepidic predominant invasive adenocarcinoma as the well-differentiated group, which had a better prognosis when compared with other subtypes. Even though micropapillary and solid predominant subtypes have significantly worse prognosis than other subtypes, they were uncommon in LCCA. Therefore we defined acinar, papillary, micropapillary, and solid subtypes in addition to mucinous adenocarcinoma as the moderately/poorly (M/P) differentiated group

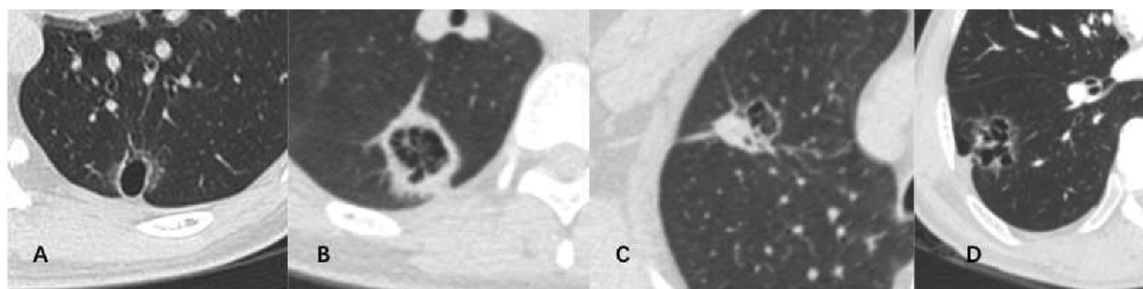


Fig. 1. Classic computed tomographic (CT) features of four morphological patterns of lung cancer associated with cystic airspace (LCCA). A. type I, mean wall thickness < 2 mm; B. type II, mean wall thickness ≥ 2 mm; C. type III: a cystic airspace with a mural nodule; D. type IV, tissue intermixed within clusters of cystic airspaces.

[10,11].

2.5. Statistical analysis

Continuous data with normal distribution were presented as means ± standard deviation (SD); non-normal variables were reported as median (interquartile range [IQR]). Categorical variables were presented as percentages. Statistical differences between the groups were analyzed using Fisher’s exact test for categorical variables and by unpaired t- or Mann-Whitney U tests for continuous variables. Variables of interest were tested on univariate binary logistic regression analysis and included in multivariable analysis if they were clinically relevant to LCCA invasiveness and statistically significant. Data was analyzed using SPSS version 21.0 (SPSS Inc., Chicago, IL, USA). Statistical significance was defined as P < 0.05.

3. Results

3.1. Characteristics of the study group

A total of 10,835 NSCLC patients underwent surgery in our hospital between 2015 and 2016. One-hundred twenty-three cases with LCCA (41 women, 82 men; mean age, 60.20 ± 9.54 years) were identified, and among them, 117 patients were diagnosed with adenocarcinoma. Only six patients were diagnosed with squamous cell carcinoma. Eighty-three (67.5%) patients were asymptomatic at diagnosis. Most patients (92.7%) underwent surgery with an observation period of less than 6 months after the first cystic lesion detection (see Table 1).

In imaging analysis of these 123 patients, 23 cases were type I (18.7%), 34 were type II (27.6%), 43 cases were type III (35.0%), and 23 cases were type IV (18.7%). Lesions were more likely to be located in the peripheral (60.2%) rather than the central (39.8%) lung. Radiographic evidence of emphysema was present in 38(30.9%) patients. Tumor stage was pre-invasive in nine (7.4%) cases but invariably advanced (93 were classified as T1, 18 were classified as T2, and three were classified as T4) in 114 (92.6%) patients. Most patients were classified as N0 (113; 91.9%). Only one patient was classified as N1 (0.8%) and nine patients as N2 (7.3%). One hundred and six (86.2%) patients underwent lobectomy, sixteen (13.0%) patients received wedge resection or segmentectomy, and only one (0.8%) patient underwent a pneumonectomy.

Based on histopathological analysis, there were four (3.3%) AIS, five (4.1%) MIA, 108 (87.7%) invasive adenocarcinoma (IA), and six (4.9%) squamous cell carcinoma (SCC) (see Table 1).

3.2. Association between LCCA imaging features and pathological invasiveness

Association between pathological invasiveness and patterns of 117 cystic lung adenocarcinomas (SCCs were excluded) are listed in Table 2. The proportion of well- and M/P-differentiated lung adenocarcinomas

Table 1
Clinicopathological characteristics of 123 patients with LCCA.

| | Number (%) |
|---|------------|
| Age | 60.20±9.54 |
| Sex (%) | |
| Female | 41(33.3) |
| Male | 82(66.7) |
| Symptoms (%) | |
| Without | 83(67.5) |
| With | 40(32.5) |
| Time between baseline and diagnosis (%) | |
| ≤6 months | 114(92.7) |
| > 6 months | 9(7.3) |
| Morphology of cyst | |
| type I | 23(18.7) |
| type II | 34(27.6) |
| type III | 43(35.0) |
| type IV | 23(18.7) |
| Lobe | |
| Right | |
| Upper | 27(22.0) |
| Middle | 12(9.8) |
| Lower | 31(25.2) |
| Left | |
| upper | 21(17.0) |
| Lower | 32(26.0) |
| Location | |
| subpleural | 74(60.2) |
| intrapulmonary | 49(39.8) |
| Emphysema | |
| Without | 85(69.1) |
| With | 38(30.9) |
| Histology (%) | |
| AIS/MIA | 9(7.4) |
| IA | 108(87.7) |
| SCC | 6(4.9) |
| T-stage | |
| AIS/MIA | 9(7.4) |
| T1 | 93(75.6) |
| T2 | 18(14.6) |
| T4 | 3(2.4) |
| N-stage | |
| N0 | 113(91.9) |
| N1 | 1(0.8) |
| N2 | 9(7.3) |
| Surgery | |
| Lobectomy | 106(86.2) |
| wedge/segmentectomy | 16(13.0) |
| Pneumonectomy | 1(0.8) |

LCCA, lung cancers associated with cystic airspace. AIS, adenocarcinoma *in situ*. MIA, minimally invasive adenocarcinoma. IA, adenocarcinoma. SCC, squamous cell carcinoma. CWN, a cystic airspace with a mural nodule.

were the same in LCCA types I and II, while in types III and IV, M/P-differentiated subtypes were more common than well-differentiated ones (type III, 15% versus 85%; type IV, 30.4% versus 69.6%).

Margins (P = 0.046) and wall components (P = 0.001) were

Table 2
Morphological LCCA patterns associated with tumor invasiveness.

| | Morphology of cyst | | | | P |
|---------------------|--------------------|---------------------|----------------------|---------------------|-------|
| | type I (N = 22) | type II (N = 32) | type III (N = 40) | type IV (N = 23) | |
| Well differentiated | 11(50.0) | 16(50.0) | 6(15.0) | 7(30.4) | 0.005 |
| M/P differentiated | 11(50.0) | 16(50.0) | 34(85.0) | 16(69.6) | |

LCCA, lung cancers associated with cystic airspace. Well differentiated: adenocarcinoma *in situ*., minimally invasive adenocarcinoma, lepidic predominant. M/P(moderately/poorly) differentiated: acinar, papillary, micropapillary, solid predominant and mucinous adenocarcinoma.

significantly associated with type I cystic lung adenocarcinoma invasiveness. Compared to well-differentiated adenocarcinomas, M/P-differentiated adenocarcinomas were more likely to have lobulated/spiculated margins (93.8% versus 50%) and part-solid components in the wall (93.8% versus 16.7%) (see Supplementary Table S1).

However in type II LCCA (similar to type I) more solid components in the wall ($P < 0.001$) predicted an aggressive histology group. Besides this feature, mean thickness and CT wall density were also predictors for tumor histological behavior (see Supplementary Table S2).

Type III was the most common LCCA pattern in our patient cohort. For the entire lesion, the maximum diameter was significantly correlated with pathological invasiveness (well-differentiated group: 21.4 ± 5.8 mm versus M/P-differentiated group: 34.4 ± 10.7 mm; $P = 0.006$) and average CT density (well-differentiated group: -585.8 ± 84.9 hounsfield units [HU] versus M/P-differentiated group: -318.0 ± 245.1 ; $P < 0.001$). Similarly, the aggressive pathological subtype group was more likely to have irregular margins (91.2% versus 33.3%; $P = 0.005$) and more solid components in the wall (47.1% versus 16.7%; $P < 0.001$). The mural nodule's size and density were significantly associated with histological subtype. The nodule's max diameter and volume were larger in the M/P-differentiated group than in the well-differentiated group (27.1 mm versus 14.8 mm; $P = 0.034$; 4.2×10^3 mm³ versus 0.5×10^3 mm³; $P = 0.007$). The nodule's CT value in the M/P-differentiated group was higher (-24.0 HU versus -404.0 HU, $P = 0.001$). Solid components in the nodule were also more common in this group (91.4% versus 28.6%; $P = 0.001$) (see Supplementary Table S3).

Typical type IVs LCCAs were rare in our patient cohort. For this morphological pattern, only components of the wall were predicted for their related pathology. In the M/P-differentiated group, the frequencies of ground-glass, part-solid, and solid component were 25%, 62.5%, and 12.5%, respectively (85.7%, 14.3%, and 0% in the mild group, respectively; $P = 0.029$) (see Supplementary Table S4).

Multivariate analysis showed the type III morphological pattern was independently associated with a higher likelihood of M/P-differentiated histological subtype (odds ratio [OR], 6.451; 95% confidence interval [CI], 1.145–36.353; $P = 0.035$) in comparison with type I LCCA. Part-solid and solid components in the wall (OR, 27.178; 95% [CI], 5.614–131.566; $P < 0.001$ and OR, 614.576; 95% [CI], 36.428–10368.608; $P < 0.001$, respectively) were associated with a higher likelihood of M/P-differentiated histological subtypes when compared with ground-glass component in wall. Irregular inner surface of the cyst (OR, 7.008; 95% [CI], 1.873–26.216; $P = 0.004$) was also an independent risk factor of M/P-differentiated histological subtypes (see Table 3).

3.3. Morphological modifications during follow-up

Thirteen patients underwent serial CT follow-up at our hospital. The average observation period was 38 months (range, 7–76 months). A total of 46 CT examinations were performed during the observation with a mean of 3.5 time points per patient. The mean time between CT

Table 3
Multivariable analysis of factors associated with tumor invasiveness for LCCAs.

| | Odds ratio (OR) | 95% confidence interval (CI) | P |
|-----------------------|-----------------|------------------------------|---------|
| Morphology pattern | | | |
| Type I | Reference | | |
| Type II | 0.310 | 0.069–1.395 | 0.127 |
| Type III | 6.451 | 1.145–36.353 | 0.035 |
| Type IV | 2.983 | 0.417–21.357 | 0.276 |
| Component of wall | | | |
| pure opacity | Reference | | |
| subsoid | 27.178 | 5.613–131.566 | < 0.001 |
| solid | 614.576 | 36.428–10368.608 | < 0.001 |
| Inner surface of cyst | | | |
| smooth | reference | | |
| Rough | 7.008 | 1.873–26.216 | 0.004 |

scans was 14 months. We identified four patterns of disease progression for these cystic airspace-related lesions (see Fig. 2). Of five type I lesions, three showed a nodule emerging from the cyst wall and became larger at a later time while two showed a circumferential thickening of the cyst wall. All three of the type II lesions ultimately became completely solid masses. All five type III lesions showed increasing attenuation and increasing mural nodule sizes. Eight cancers showed a decrease in cystic airspace size along with increasing solid elements. Only one case showed cyst enlargement.

3.4. Mutational analysis

Among the four LCCA patterns, 52.9% (45/85) lung cancers tested positive for epidermal growth factor (EGFR) mutations. There was not much difference among different patterns. Kirsten rat sarcoma viral oncogene homolog (KRAS) mutations and anaplastic lymphoma kinase (ALK) were both rarely detected in LCCAs (6%, 5/83, and 1.3%, 1/78, respectively) (see Table 4).

4. Discussion

Our study first investigated the correlation of LCCA imaging characteristics with pathological invasiveness and gene status. In general, more solid components in the wall and irregular inner surface of cysts were two predictors of M/P-differentiated histological subtypes. Separately, in type II, wall thickness and density was also associated with pathological invasiveness. In type III, mural nodule size and density were also significantly differentiating factors. In serial CT follow-up, emerging mural nodules, increasing attenuation and size of mural nodule, and thickening of a cyst wall should raise clinical suspicion. EGFR mutation rate was not significantly different among the four types of LCCA.

The incidence of LCCAs was 1.1% in our surgical lung cancer series, which is similar to prior studies. The reported incidence of LCCA from the prior studies was 3.7% in a lung cancer-screening cohort [12]. Sex difference was apparent in LCCA, in which male patients constituted the patient majority. Araki et al. [13] demonstrated that emphysema appeared in 12.5% (25/200) of benign pulmonary cysts, while in lung cancer patients, the ratio increased 47%–76% [14]. Previous evidence has suggested that emphysema can increase the risk of lung cancer up to four to five times [15]. A hypothetical explanation for this finding suggested that in emphysema patients, cysts might interfere with ventilation and lung clearance, which could cause carcinogen deposition [4]. In our study cohort, presence of emphysema in patients with LCCAs was 30.9% (38/123), which was much lower than the previously presented proportion. A possible explanation for this difference may have resulted from the exclusion criteria (which excluded many patients with emphysema). LCCAs are more likely to appear in the peripheral area of all lobes. In this situation, the differential diagnosis includes bullae and paraseptal emphysema [16].

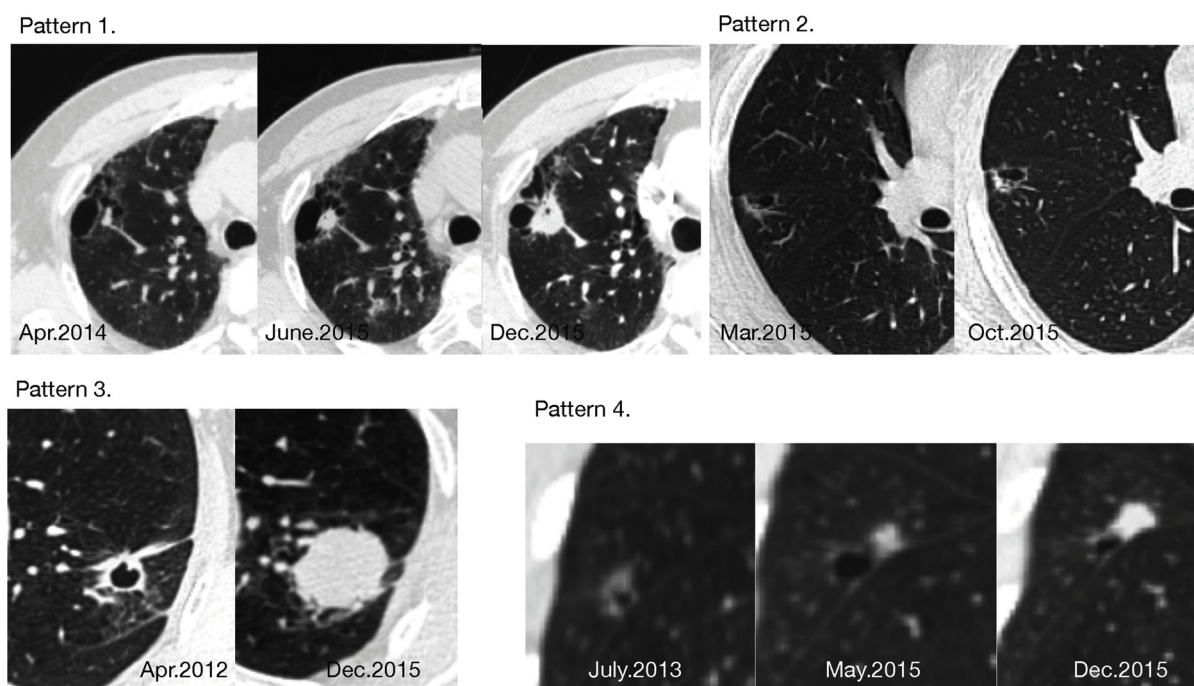


Fig. 2. Four patterns of disease progression. Pattern 1 shows a nodule emerging from the cyst wall that enlarged later during the follow-up. Pattern 2 shows wall thickening of the initial thin wall. Pattern 3 shows a thick-walled type cyst replaced by a solid mass. Pattern 4 shows an increase in mural nodule attenuation and size.

Table 4
Mutational analysis for four patterns of LCCA.

| | | Type I | Type II | Type III | Type IV | P |
|------|---------------|----------|-----------|-----------|----------|-------|
| EGFR | wild type | 7 (50) | 10 (47.6) | 15 (42.9) | 8 (53.3) | 0.912 |
| | mutation | 7 (50) | 11 (52.4) | 20 (57.1) | 7 (46.7) | |
| KRAS | wild type | 14 (100) | 18 (90) | 31 (91.2) | 15 (100) | |
| | mutation | 0 | 2 (10) | 3 (8.8) | 0 | |
| ALK | wild type | 14 (100) | 19 (100) | 29 (96.7) | 15 (100) | |
| | rearrangement | 0 | 0 | 1 (3.3) | 0 | |

EGFR, epidermal growth factor; KRAS, Kirsten rat sarcoma viral oncogene homolog; ALK, anaplastic lymphoma kinase.

There are several systems for LCCA classification. The morphology-based classification system was first described in 2006 by Maki et al. [17]. Three patterns of CT appearances were identified: (a) type I: nodule or mass extruding from the bullous lumen ($n = 11$); (b) type II: nodule or mass confined within the bullous lumen ($n = 2$); and (c) type III (CWN): soft-tissue density extending along the bullous wall ($n = 7$). It was modified by Mascacchi et al. [9] in 2015. They added a new type of LCCA, which presents as soft tissue density intermixed within clusters of cystic airspaces. Following this version, Fintelmann et al. [6] developed a more comprehensive classification system, which consisted of three parts: (a) types of cystic lesions; (b) consistency of a nodule, mural nodule, or wall thickening; and (c) internal cystic airspace separations. Cystic lesions were divided into thin-walled (maximum wall thickness of 1 mm), thick-walled (wall thickness > 1 mm), and a cystic airspace with an endophytic nodule. Consistency depended on the lesion's solid components. Unilocular and multilocular were used to describe the cyst's internal structure.

Based on previous studies and our results, four morphological LCCA patterns were identified in the present study: (a) type I (thin-walled type) ($n = 23$); (b) type II (thick-walled type) ($n = 34$); (c) type III (CWN) ($n = 43$); and (d) type IV (mixed type) ($n = 23$). Similar to other studies, type III was the most common type followed by type II. The proportion of types I and IV in our study were approximately the same.

In the International Association for Lung Cancer/American Thoracic Society/ European Respiratory Society (IASLC/ATS/ERS) classification,

the terms AIS and MIA indicate cases in which a patient undergoes a complete resection, he/she will have 100% or near 100% disease-specific survival. Among the invasive adenocarcinoma subtypes, lepidic predominant invasive adenocarcinoma has the best prognosis compared to other subtypes [11]. Therefore, recognizing cancers with different invasiveness when they manifest with different radiological features can be highly useful in management and prognostic decisions.

In pulmonary nodules, it is well known that lesion size, solid component, margin, air bronchogram, and pleural tag can be used to accurately distinguish pre-invasive lesions from invasive adenocarcinomas [18,19], whereas it appears much more difficult to create a universal diagnostic imaging model for LCCAs because of the diverse morphology of these lesions. Thus, in this study, we used different CT-based parameters to evaluate each type of LCCA. In general, as indicated in ground glass nodules, solid proportion also plays a considerable role in prediction of LCCA invasiveness. The differentiating CT features for pulmonary nodules can also be applied in type III mural nodules. However, unlike nodule size, size of cyst had little predictive value. Margins of cystic lesions can be divided into smooth, lobulated, and spiculated. In common pulmonary nodules, malignant ones often present with irregular, spiculated, and ill-defined margins [19]. It is the same in LCCA aggressive lesions, which are more likely to have ill-defined margins. Based on our results, it seems reasonable that protocols for non-small cell lung cancer can be used to guide the invasiveness of LCCA.

It should be noticed that the type III morphological pattern was an independent risk factor for M/P-differentiated subtypes in multivariate analysis. The pathologically invasive type III traits as shown in our study are in line with those in a report by Toyokawa [20], which prompt us that type III represents a distinct group of pulmonary nodules with higher pathologic invasiveness that needs aggressive treatment.

Another finding of our study was the temporal evolution of LCCA. According to Lindell et al.'s five-year lung cancer screening experience, CT appearance changes including increasing attenuation and/or irregularities or spiculation are highly indicative of lung cancer [21]. This is in contrast to benign pulmonary cysts, which mostly remain unchanged or slightly increase in size over time [13]. Pulmonary cysts indicative of lung cancers usually develop wall thickening and/or mural

nodularity during follow up [4,9]. In our 13 patients over observation, the wall of five patients' cystic airspace was initially thin (average thickness < 2 mm) but over time, two of these patients' cystic airspaces became thicker, and three transformed into type III. The majority of patients in Mascalchi's report [9] also developed in this way. This might be a warning sign of *de novo* carcinogenesis in the preexisting benign bullae and may be preceded by new cystic airspaces or nodules [6]. Our study documents the independence of mural nodule emergence and increase in wall thickening. Cystic airspaces generally were reduced in size ($n = 8$) and in three type II lesions were ultimately replaced by solid components. The replacement of the cystic airspace by soft tissue attenuation indicates that a cystic airspace is part of lung cancer [6]. There was only one case in our study showing cyst enlargement, while in Mascalchi's and Fintelmann's studies, cyst enlargement was not a negligible group, presumably reflecting a valve mechanism on the distal airway connected with the cystic airspaces [6,9].

Mutational analysis revealed EGFR mutations as the predominant alterations in every morphological subtype. Only a few types II and III patients showed KRAS mutations. This finding is similar to Guo et al.'s [12] study. Interestingly, Fintelmann et al. [6] reported that 64% of adenocarcinomas tested positive for a KRAS alteration. The difference of prevalent mutations may be due to the difference in genotype between Asians and Caucasians [22,23]. EGFR mutations have been shown to be involved in the initial tumorigenesis process, are frequently detected in early stage lung adenocarcinoma and associated with the lepidic pattern [24]. In our study, most LCCAs presented in stage I, and the three most frequent histological subtypes were lepidic, acinar, and papillary.

We recognize some limitations of our study. First, it was a retrospective study, and this implied missing data, such as smoking history. This prevented us from exploring the association between smoking and LCCA. Second, reconstruction kernel is one of the most important parameters that affect the image quality of lung CT scans. In the present study, we used different reconstruction kernels for the patients, which inevitably influenced the morphological features of LCCA. Third, serial CT follow-up is not adequate, both the number of our patients and the observation period cannot compare to the studies conducted by Mascalchi and Fintelmann [6,9]. Fourth, four possible pathogenesis of cyst formation has been proposed by Fintelmann [6], but we were not able to perform histological analysis to validate them.

5. Conclusion

In summary, our observational study demonstrated that thin- and thick-walled (types I and II, respectively), CWN (type III), and mixed (type IV) are four common morphological subtypes of LCCAs. Among them, type III accounted for the biggest proportion of types and presented the most aggressive behavior. Wall component was an important factor for determining LCCA's pathological invasiveness. A change in the morphological features of the cyst wall or mural nodule should raise suspicion for cancer. EGFR mutations were the predominant genetic alterations.

Funding

This work was supported by Shanghai Shen Kang Hospital Development Center [grant numbers16CR2016A].

Conflict of interest

All authors declare that there are no relationships or activities that could influence the submitted work.

Acknowledgements

We would like to show our gratitude to Dr. Dana Ferrari-Light for her assistance with the English and grammar check that greatly

improved the manuscript.

Appendix A. Supplementary data

Supplementary material related to this article can be found, in the online version, at doi:<https://doi.org/10.1016/j.lungcan.2019.05.012>.

References

- [1] J.H. Austin, N.L. Müller, P.J. Friedman, D.M. Hansell, D.P. Naidich, M. Remy-Jardin, et al., Glossary of terms for CT of the lungs: recommendations of the nomenclature committee of the Fleischner society, *Radiology* 200 (1996) 327–331.
- [2] D.M. Hansell, A.A. Bankier, H. MacMahon, T.C. McLoud, N.L. Müller, J. Remy, et al., Fleischner society: glossary of terms for thoracic imaging, *Radiology* 246 (2008) 697–722.
- [3] S. Sheard, J. Moser, C. Sayer, K. Stefanidis, A. Devaraj, I. Vlahos, Lung cancers associated with cystic airspaces: underrecognized features of early disease, *Radiographics* 38 (2018) 704–717.
- [4] A.O. Farooqi, M. Cham, L. Zhang, M.B. Beasley, J.H. Austin, A. Miller, et al., International Early Lung Cancer action Program, lung cancer associated with cystic airspaces, *AJR Am. J. Roentgenol.* 199 (2012) 781–786.
- [5] E.T. Scholten, N. Horeweg, H.J. de Koning, R. Vliegthart, M. Oudkerk, W.P. Mali, et al., Computed tomographic characteristics of interval and post screen carcinomas in lung cancer screening, *Eur. Radiol.* 25 (2015) 81–88.
- [6] F.J. Fintelmann, J.K. Brinkmann, W.R. Jeck, F.M. Troschel, S.R. Digumarthy, M. Mino-Kenudson, et al., Lung cancers associated with cystic airspaces: natural history, pathologic correlation, and mutational analysis, *J. Thorac. Imaging* 32 (2017) 176–188.
- [7] C.F. Mountain, Dresler CM: regional lymph node classification for lung Cancer Staging, *Chest* 111 (1997) 1718–1723.
- [8] A. Snoeckx, P. Reyntjens, D. Desbuquoit, M.J. Spinhoven, P.E. Van Schil, J.P. van Meerbeeck, et al., Evaluation of the solitary pulmonary nodule: size matters, but do not ignore the power of morphology, *Insights Imaging* 9 (2018) 73–86.
- [9] M. Mascalchi, D. Attinà, E. Bertelli, M. Falchini, A. Vella, A.L. Pegna, et al., Lung Cancer Associated with cystic airspaces, *J. Comput. Assist. Tomogr.* 39 (2015) 102–108.
- [10] T. Eguchi, K. Kadota, B.J. Park, W.D. Travis, D.R. Jones, P.S. Adusumilli, et al., The new IASLC-ATS-ERS lung adenocarcinoma classification: what the surgeon should know, *Semin. Thorac. Cardiovasc. Surg.* 26 (2014) 210–220.
- [11] W.D. Travis, E. Brambilla, M. Noguchi, A.G. Nicholson, K.R. Geisinger, Y. Yatabe, et al., International association for the study of lung Cancer/American thoracic Society/European respiratory society international multidisciplinary classification of lung adenocarcinoma, *J. Thorac. Oncol.* 6 (2011) 244–285.
- [12] J. Guo, C. Liang, Y. Sun, N. Zhou, Y. Liu, X. Chu, Lung cancer presenting as thin-walled cysts: an analysis of 15 cases and review of literature, *Asia J. Clin. Oncol.* 12 (2016) e105–e112.
- [13] T. Araki, M. Nishino, W. Gao, J. Dupuis, R.K. Putman, G.R. Washko, et al., Pulmonary cysts identified on chest CT: are they part of aging change or of clinical significance? *Thorax* 70 (2015) 1156–1162.
- [14] C. Mouronte-Roibas, V. Leiro-Fernandez, A. Fernandez-Villar, et al., COPD, emphysema and the onset of lung cancer. A systematic review, *Cancer Lett.* 382 (2016) 240–244.
- [15] J.P. de Torres, G. Bastarrika, J.P. Wisnivesky, A.B. Alcaide, A. Campo, L.M. Seijo, et al., Assessing the relationship between lung Cancer risk and emphysema detected on low-dose CT of the chest, *Chest* 132 (2007) 1932–1938.
- [16] S. Raoof, P. Bondalapati, R. Vidyula, J.H. Ryu, N. Gupta, S. Raoof, et al., Cystic lung diseases: algorithmic approach, *Chest* 150 (2016) 945–965.
- [17] D. Maki, M. Takahashi, K. Murata, S. Sawai, S. Fujino, S. Inoue, Computed tomography appearances of bronchogenic carcinoma associated with bullous lung disease, *J. Comput. Assist. Tomogr.* 30 (2006) 447–452.
- [18] Sang Min Lee MD, Chang Min Park MD, Jin Mo Goo MD, Invasive Pulmonary adenocarcinomas versus Preinvasive lesions appearing as ground-glass nodules: differentiation by using CT Features, *Radiology* 268 (2013) 266–273.
- [19] A.N. Khan, H.H. Al-Jahdali, K.L. Irion, M. Arabi, S.S. Koteyar, Solitary pulmonary nodule: a diagnostic algorithm in the light of current imaging technique, *Avicenna J. Med.* 1 (2011) 39–51.
- [20] G. Toyokawa, M. Shimokawa, Y. Kozuma, T. Matsubara, N. Haratake, Takamori S. Invasive features of small-sized lung adenocarcinoma adjoining emphysematous bullae, *Eur. J. Cardiothorac. Surg.* (2017) 1–7.
- [21] R.M. Lindell, T.E. Hartman, S.J. Swensen, J.R. Jett, D.E. Midthun, H.D. Tazelaar, et al., Five-year lung Cancer, Screening experience:CT appearance, growth rate, Location, and histologic features of 61 lung cancers, *Radiology* 242 (2007) 555–562.
- [22] K.C. Arbour, E. Jordan, H.R. Kim, J. Dienstag, H.A. Yu, F. Sanchez-Vega, et al., Effects of Co-occurring genomic alterations on outcomes in patients with KRAS-Mutant non-small cell lung Cancer, *Clin. Cancer Res.* 24 (2018) 334–340.
- [23] V. Morales-Oyarvide, M. Mino-Kenudson, High-grade lung adenocarcinomas with micropapillary and/or solid patterns: a review, *Curr. Opin. Pulm. Med.* 20 (2014) 317–323.
- [24] J. Dai, J. Shi, A.K. Soodeen-Laloo, P. Zhang, Y. Yang, C. Wu, et al., Air bronchogram: a potential indicator of epidermal growth factor receptor mutation in pulmonary subsolid nodules, *Lung Cancer* 98 (2016) 22–28.